NICOLAUS COPERNICUS UNIVERSITY IN TORUŃ

Bulletin of Geography. Physical Geography Series, No. 30 (2026): 51–71
http://doi.org/10.12775/bgeo-2026-0004

Monitoring agricultural drought based on optical remote sensing data

Abdur Rahim Mozomdar[1]a*, Noshin Nawar Jahan[2], Rezaul Roni[3]

[1,2]Beihang University Hangzhou International Innovation Institute, A Remote Sensing and Geo-Information System, Space Technology Application, Hangzhou, China

[3]Jahangirnagar University, Department of Geography and Environment, Dhaka, Bangladesh

E-mail: armozomdar@gmail.com

[a]https://orcid.org/0009-0008-4940-8388

Abstract. Agricultural drought is a result of prolonged rainfall deficits affecting rice productivity. Agriculturally dependent regions are more vulnerable to agricultural drought. Therefore, drought monitoring is essential for effective agricultural management. This study aimed to investigate the drought variability of Rajshahi, Bangladesh utilizing optical remote sensing data from Landsat during 2000 to 2024, excluding 2007 due to technical faults in satellite imageries. This drought assessment used the Vegetation Health Index (VHI), which combines the Vegetation Condition Index (VCI) and the Temperature Condition Index (TCI), during pre-monsoon (March–May) and post-monsoon (October–November) seasons. The Standardized Precipitation Evapotranspiration Index (SPEI) was also used for cross-validation of areas affected by meteorological and agricultural drought. This study reveals that the "slightly dry" category of drought was predominant in all the districts for both seasons, where districts like Chapainawabganj, Pabna, Rajshahi and Sirajganj exhibited a significantly higher frequency of "dry" and "slightly dry" drought conditions. The Mann–Kendall test found no statistically significant trend of VHI for 24 years, indicating that drought has no linear pattern of occurrence. The cross-tabulation between SPEI and VHI showed a moderate agreement between drought categories, but a good relationship was found in normal conditions of drought from both indices. This suggests that meteorological drought may not be the only cause of agricultural drought; climate variables and agricultural practice have a great influence too.

Key words:
Agricultural drought,
Remote Sensing,
VHI,
SPEI,
GEE

Introduction

It is assumed that the journey of climate change research began in the 17th century with an Italian scientist (Iafrate et al. 2017). In recent years, climate change has exacerbated several natural disasters, especially those that affect agriculture, leading to food insecurity (Jiménez-Donaire et al. 2020). The consequences of climate change are miscellaneous and vary from global to regional, which sometimes can lead to various catastrophic events like "drought" (Loukas et al. 2008). Climate change is expected to worsen droughts and increase their frequency globally, especially in semi-arid regions with high water stress (Cook et al. 2018). Drought is usually a long-term water scarcity where precipitation is exceeded by evapotranspiration (Varghese et al. 2021). This natural disaster occurs frequently, harming human societies (Cook et al. 2018; Dai et al. 2018; Mukherjee et al. 2018; Kamruzzaman et al. 2019; Gaitán et al. 2020) and leaves a long-lasting effect on the socio-economic system of a region (Arnell 2007), affecting millions of people annually (Gaitán et al. 2020). However, the impacts of drought depend on its intensity, duration and extent of climatic irregularity and on the vulnerability of human systems (Arnell 2007). According to the IPCC

(Intergovernmental Panel on Climate Change), global drought occurrences may worsen in the twenty-first century because of climatic instability (Arnell 2007; Gaitán et al. 2020).

Although drought is caused by precipitation deficits, it can also occur in regions with high precipitation because it is additionally affected by temperature, evapotranspiration, relative humidity, soil types, wind and vegetation (Gaitán et al. 2020). By raising surface temperatures and evapotranspiration and lowering precipitation, climate change has increased the severity and frequency of meteorological drought (Varghese et al. 2021). Agricultural drought occurs when a meteorological drought reduces soil moisture and hinders plant development (Berg and Sheffield 2018). This drought deprives plant roots of moisture, causing crop growth stress, yield reduction or crop failure (Sruthi and Aslam 2015). The agriculture sector is most vulnerable to droughts since crops rely on rainfall and temperature for their growth and development (Wilhite 1993). Rainfall anomalies and temperature rises that diminish soil moisture both reduce agricultural productivity (Sruthi and Aslam 2015). Among meteorological disasters, agricultural drought causes the most socio-economic losses to the world because it can affect food production and water delivery systems and more (Araneda-Cabrera et al. 2021). Even among regions that share similar water limitations, drought intensity may vary depending on the number of hazard-affected bodies exposed to natural disasters, their nature, and people's response to drought (Pei et al. 2019).

Drought affects more people than any other natural disasters by lasting for a longer period of time (Kuj and Kam 2021). It is widespread and more frequent in semi-arid environments (Sandeep et al. 2021) and can worsen food shortages in developing countries (Begna et al. 2022). According to Pequeno et al. (2021), drought in Africa and Southern Asia will reduce global wheat production by the middle of this century. In Bangladesh, agricultural drought is a matter of concern, notably in terms of agricultural productivity (Mondol et al. 2017), since it occurs frequently – on average every 2.5 years (Sultana et al. 2021). This country has suffered from this calamity for decades, causing the loss of ~1.5 million tons of crops each year (Prodhan et al. 2020). Drought is becoming more threatening to this region, since it results in food insecurity by affecting agricultural productivity (Mahmud et al. 2021). Based on the nature of drought, the northern, western, north-western and south-western regions of the country are most vulnerable to drought (Islam et al. 2019). The north-western and south-western parts of this country are facing severe drought because of the particularity of their regional geo-climatic and human-induced factors (Habiba et al. 2013). Agricultural drought is characterized by a timeframe that is pre-monsoon (March–May) and post-monsoon (October–November) (Habiba et al. 2013). Pre-monsoon drought is associated with inadequate rainfall (Alamgir et al. 2015), whereas post-monsoon drought is caused by insufficient moisture content in the soil (Akter and Rahman 2012).

Drought is complicated to identify and predict because of its complex mechanisms (Zhai et al. 2020) and is the least studied among all natural disasters (Araneda-Cabrera et al. 2021) due to the insufficiency of historical data (Varghese et al. 2021). Bangladesh has been monitoring drought traditionally (Prodhan et al. 2020) using methods like the Standard Precipitation Index (SPI), a method for quantifying meteorological drought (Aswathi et al. 2018) that is further used to examine agricultural drought. Another traditional method involves ground-based measurement of soil moisture (Cheng et al. 2024). However, traditional assessment methods are unreliable in terms of accuracy (Salite 2019), time-consuming and labor-intensive (Cheng et al. 2024). Thus, satellite remote sensing is an essential data source for measuring drought duration, magnitude, frequency and extent (Sholihah et al. 2016) more accurately than by traditional methods (Bayable and Gashaw 2021). Integrating satellite data with meteorological data is an effective method for accurately monitoring agricultural drought to provide timely drought management while minimizing the dependence on remote sensing data alone (Sun et al. 2017). Studies have used such an improved approach for detecting and assessing drought severity in a diverse climatic zone like China (Dabrowska-Zielinska et al. 2020; Jiang et al. 2025). Researchers use vegetation indices like Normalized Difference Vegetation Index (NDVI), Normalized Difference Water Index (NDWI), Enhanced Vegetation Index (EVI), Vegetation Condition Index (VCI), Vegetation Health Index (VHI) and Normalized Difference Drought Index (NDDI) (Measho et al. 2019; Bayable and Gashaw 2021) to assess drought conditions (Sruthi and Aslam 2015). Remote sensing and GIS technologies reduce dependency on in-situ observation in analyzing agricultural drought (Wu et

al. 2021). Therefore, drought intensity needs to be mapped effectively in order to better understand its effect on agriculture productivity (Mondol et al. 2017).

Research on drought mainly focuses on identifying its impact on humans and the environment and on developing resilience strategies to reduce drought impact (Varghese et al. 2021). Some drought indices are designed to evaluate drought severity, frequency, duration and extent (Islam et al. 2019), whereas others measure drought consequences (Mukherjee et al. 2018). Vegetation indices (VIs) such as NDVI, VCI and NDWI can determine agricultural drought (Bartold et al. 2024; Menegbo 2024; Tonyaloğlu and Atak 2024). However, there are shortcomings in using NDVI (Bohon 2024; Farmonaut 2024), NDWI (Farmonaut 2024) and VCI (Mustapha and Zineddine 2024) for drought monitoring. These can be addressed by utilizing the vegetation health index (VHI), because it has a robust link with crop development (Wu et al. 2020). VHI considers VCI and the temperature condition index (TCI) to calculate drought, where both parameters are estimated from NDVI and land surface temperature (LST) (Sholihah et al. 2016). Therefore, this study utilized VHI to observe the agricultural drought variability of Rajshahi division in Bangladesh during pre-monsoon (March–May) and post-monsoon (October–November) from 2000 to 2024 using multi-spectral optical remote sensing data. This index is among the most widely used vegetation indices for monitoring agricultural drought (Yang et al. 2011; Kloos et al. 2021). Some specific objectives were chosen to attain the goal of this research, namely 1) determining the pre-monsoon and post-monsoon agricultural drought condition, variability and its spatial distribution over the selected area using VHI; 2) assessing the temporal trends of VHI by analyzing drought frequency on different districts of Rajshahi division; and 3) comparing the drought from VHI with SPEI to observe whether meteorological drought influenced agricultural drought.

Study area

The study area for this research was selected based on a pre-analysis of drought. Because not all regions of Bangladesh are familiar with drought, it is very difficult to select an area randomly for drought assessment. When a region faces meteorological drought, it may gradually extend to agricultural drought. Meteorological drought can be assessed with the standardized Precipitation Evapotranspiration Index (SPEI), an upgraded form of the Standardized Precipitation Index (SPI). Therefore, to facilitate appropriate agricultural drought analysis, this study first calculated SPEI to identify which areas frequently faced meteorological drought.

The monthly SPEI was measured over the eight divisions of the country throughout the study years. Figure 1 shows that all the divisions in the western part (Rangpur, Rajshahi and Khulna) faced more frequent meteorological drought from the year 2000 to 2024 compared to the other five divisions. Among those three divisions, the Rajshahi division was more vulnerable to meteorological drought in both pre-monsoon and post-monsoon. Therefore, the Rajshahi division (Fig. 2), which includes eight divisions (Bogra, Chapai, Joypurhat, Naogaon, Natore Pabna, Rajshahi, Sirajganj), was selected as the study area for assessing the drought variability by remote sensing method.

The Rajshahi division in the north-western part of Bangladesh covers 17,974.68 km^2. This region is characterized by high temperatures and tropical dry and wet climatic conditions. In almost all seasons, Rajshahi division undergoes the maximum temperature as compared to other parts of the country (Alam et al. 2024). However, the temperature can

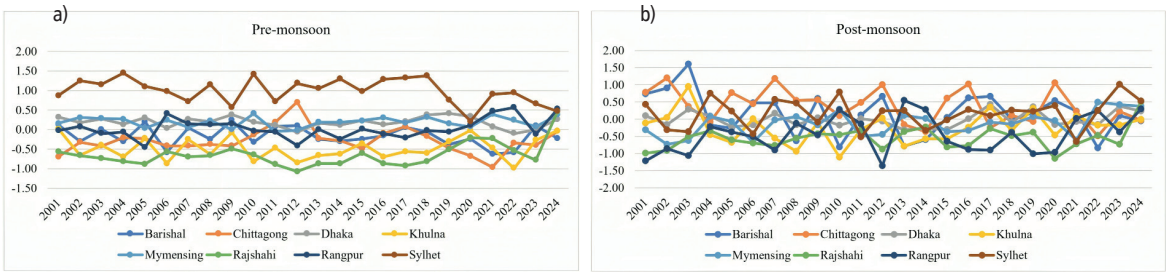

Fig. 1. Yearly mean SPEI trend: (a) Pre-monsoon season, (b) Post-monsoon season

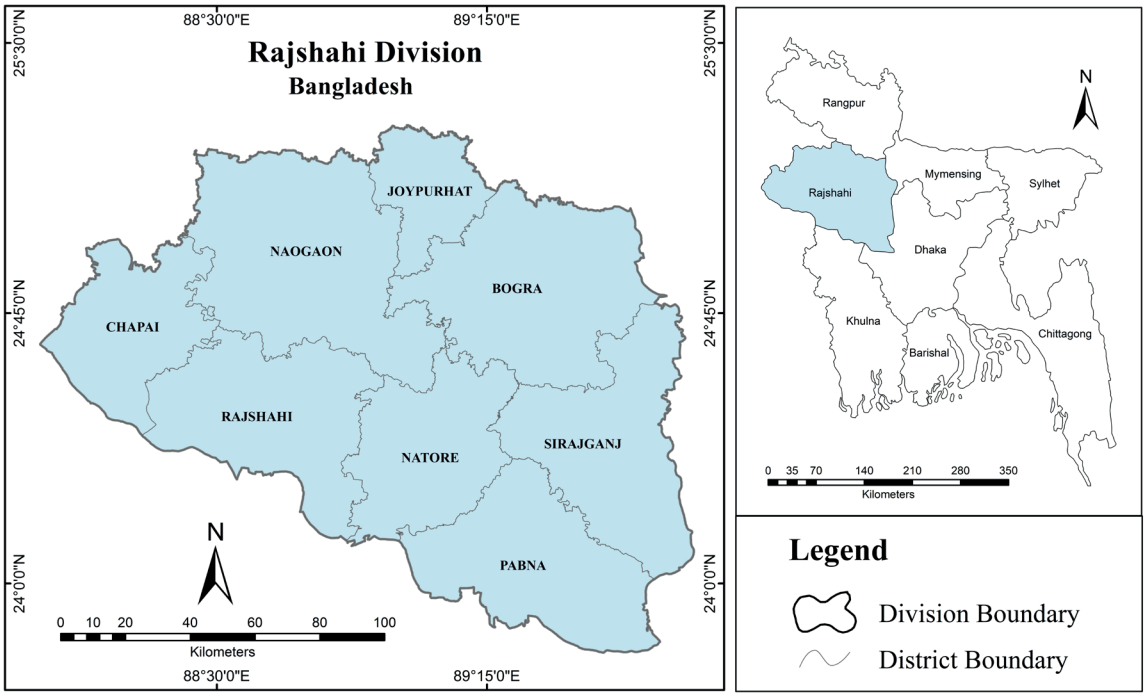

Fig. 2. Study area showing Rajshahi Division

exceed 35 °C during the month of April. In January, the temperature drops to that of other regions of Bangladesh (Data, n.d.). Rajshahi receives ~1,600 mm of rainfall annually, which is very low in contrast to other parts of the country, where average annual rainfall is 2,300 mm (Binte Mahtab and Mostafa Khan 2018). Rainfall mainly occurs during the monsoon season, which accounts for ~60% of total annual rainfall. But the trend of yearly rainfall in Rajshahi is decreasing according to a study from 2021 (Sunny et al. 2021). The relative humidity of Rajshahi is also increasing each year (Ferdous and Baten 2012). The region has already experienced multiple droughts (Haque et al. 2019) because of extreme weather conditions like insufficient rainfall, high air temperature and high relative humidity, and the frequency of drought is growing yearly – particularly during monsoon season.

Materials and methods

The study applied both satellite remote sensing data (for agricultural drought) and climatic data (for meteorological drought) to provide a more comprehensive and precise analysis of drought. The optical remote sensing data were used to assess the agricultural drought using VHI, and climatic data were used for calculation of meteorological drought by SPEI.

Satellite data

The monitoring of agricultural drought using remote sensing was based entirely on aerial photography. This study used satellite images from different Landsat satellite missions as the secondary source of data. The multispectral images from Landsat programs can detect any changes in vegetation conditions over a large area, which is crucial for agricultural drought monitoring. Landsat 5, Landsat 7, Landsat 8 and Landsat 9 were used in different years to overcome different issues, such as image availability and cloud cover. Landsat 7 satellite captured images from 1999 to 2021, and Landsat 8 provides images from 2013 to the present day. So, for the first section of this study (2000 to 2012), images from Landsat 7 were planned to be used. Since Landsat 7 had some sensor

issues, Landsat 5 images were used to replace that problematic imagery for this period. The year 2007 showed abrupt measurement by VHI because of excessive cloud cover in both Landsat 5 and Landsat 7 imagery. Thus, this year was not considered for agricultural drought calculation. From 2013 to 2020, Landsat 8 images were utilized, and, from 2021 to 2024, images collected by Landsat 9 were used as the final part of this study. Table 1 shows the uses of different satellites in different years. However, not all the bands of these two Landsat programs were needed to calculate the Vegetation Health Index (VHI); only the Red, Near Infrared and Thermal bands were used. Aggregation of these three bands from Landsat helped to determine the vegetation condition and drought variability of the study area.

Landsat satellite images were gathered and processed using the Google Earth Engine (GEE), a powerful cloud-based platform for processing satellite data. The radiometric and geometric corrections for Landsat imageries had already been preprocessed in GEE, meaning the study did not have to go through any of that preprocessing. Since the seasons selected for this study were affected by the cloud coverage for the satellite imageries, the cloud-masking process was completed for all cloudy images using cloud-masking algorithms in GEE. The removing of clouds and shadows from the satellite images ensured that images were reliable for a robust drought analysis. Therefore, the computation and export of vegetation health conditions during the study period were completed by the VHI on the GEE platform.

Meteorological data

The objectives of this study were not limited to the assessment of agricultural drought using remote sensing methods but also included exploring the meteorological drought contribution to agricultural drought, which drives this study to use some climatic variables, viz, rainfall and evapotranspiration. Rainfall and evapotranspiration were specifically used for calculating the SPEI, a method that can measure meteorological drought severity. All the climatic data used during this study were retrieved from the global terrestrial dataset, TerraClimate. This dataset provides different significant meteorological data with a high spatial resolution of four kilometers, combining WorldClim, Climatic Research Unit Time series version 4.0 (CRU Ts 4.0) and the Japanese 55-year Reanalysis (JRA55). TerraClimate uses a water balance model to produce a monthly water balance dataset, offering meteorological data for the global terrestrial body. The climatic data provided by this dataset are well-accepted and accurate because the data are validated using several station-based observations.

The collection of climatic data from TerracClimate was quite simple because they are free to access. After downloading the yearly composited data, the NetCDF file was converted into a spreadsheet, and each month's data was extracted. The SPEI calculation was then completed using Python programming from the converted rainfall and evapotranspiration data.

Table 1. Summary of selected dataset

Dataset	Variables	Spatial resolution	Mission period	Years used
TerraClimate	Temperature, Rainfall, Evapotranspiration	4 km	1958–present	2000–2024
Landsat 5	Red, NIR, TIRS	30 m	1984–2013	2004–2006, 2008–2011
Landsat 7	Red, NIR, TIRS	30 m	1999–2021	2000–2003, 2012
Landsat 8	Red, NIR, TIRS	30 m	2013–present	2013–2020
Landsat 9	Red, NIR, TIRS	30 m	2021–present	2021–2024

Note: Red – Red band; NIR – Near-infrared band; TIRS – Thermal infrared sensor band

Table 2. Category of meteorological drought from SPEI

SPEI Range	Drought Class
≤ -1.00	Dry
-1.00 to < -0.50	Slightly dry
-0.50 to < 0.50	Normal
0.50 to < 1.00	Slightly wet
≥ 1.00	Wet

Methods

The processing of satellite imagery for this study was conducted using the Google Earth Engine (GEE) platform, and the map-making was performed in ArcMap version 10.8. The Python language was also used for converting the NetCDF into an Excel sheet, the calculation of SPEI, trend analysis and SPSS for making a confusion matrix.

Processing of meteorological data

The meteorological data were collected for this study using the TerraClimate dataset (https://www.climatologylab.org/). The monthly data were directly downloaded from the TerraClimate website in NetCDF format, which was then converted into the spreadsheet. The conversion was completed using Jupyter Notebook, a Python interpreter. For each climatic variable, one Excel file was created that consists of the location of each pixel (latitude and longitude) and pixel value of that location for that variable from 2000 to 2024. These files of precipitation and potential evapotranspiration were then used for SPEI calculation.

SPEI calculation

Meteorological drought was calculated using the Standardized Precipitation Evapotranspiration Index (SPEI) method. The one-month SPEI was calculated from precipitation (P) and potential evapotranspiration (PET) data using a Python interpreter. The data were in NetCDF format, which was then converted into a spreadsheet. To measure the SPEI, the water balance first needed to be calculated by subtracting the potential evapotranspiration from precipitation.

$$D = P - PET$$

In the above equation, P represents the precipitation; PET represents potential evapotranspiration and D is the calculated water balance. The water balance can be aggregated over different time scales (e.g., 1-month, 3-month or 6-month) to calculate different months' SPEI. But this study did not accumulate water balance, because it calculated only 1-month SPEI. Then, the Log-Logistic Distribution was used for fitting the water balance in SPEI. Though there are some other distribution methods, the Log-Logistic Distribution is the default for SPEI calculation. Finally, this distribution was converted into a standard normal distribution for the calculation of monthly SPEI. Because this study analyzed the pre-monsoon and post-monsoon drought, the SPEI for these seasons was then separated into two seasons.

The mean value of SPEI for pre-monsoon and post-monsoon was used to compare against agricultural drought. The drought ranges from SPEI and VHI differed from one another; therefore, a common drought classification was created for both meteorological and agricultural drought. The categorization of drought from SPEI was ranked in five groups, as shown in Table 2. Each of the groups indicated the severity of meteorological drought for a specific SPEI range, where the lower the SPEI value, the higher the drought severity. The months for pre-monsoon and post-monsoon are March to May and October to November, respectively.

Calculation of VHI and drought-affected area

This study used the Vegetation Health Index (VHI) for measuring the agricultural drought of Rajshahi Division using the GEE platform. VHI was developed by Kogan to analyze agricultural drought by examining the comprehensive effects of agricultural practices, climate, precipitation and soil moisture of a particular location (Bayable and Gashaw 2021). In the GEE data catalog, Landsat has three types of

datasets for each mission, namely Raw Images, Top of Atmosphere (TOA) and Surface Reflectance (SR). For the calculation of VHI, this study used the Tier 1 SR dataset of the Landsat program, because it is the most processed and Tier 1 has higher-quality images than Tier 2. After adding the desired dataset into the GEE platform, the area of interest was clipped using the Rajshahi boundary shapefile.

Each image from 2000 to 2024 for the two seasons was processed individually. Initially, cloud- and shadow-masking algorithms were used to remove the cloud and shadows from each image. To remove the unwanted pixels of cloud and shadow, we used the Quality Assurance (QA_PIXEL) band of the Landsat program, which stores information about the quality of each pixel. The "Bitwise AND" operator was used for isolating pixels of cloud (bit 3) and shadow (bit 4). Then a function called "updateMask()" was applied to remove cloud and shadow pixels from the image after combining both masks (bit 3 and bit 4) in GEE.

Cloud-masking resulted in some gaps in the image by removing clouds and shadows from affected pixels. The focalMean, an interpolation function of GEE, was used to fill or minimize some of those gaps by averaging the values of the pixels nearest to the missing pixel. Subsequently, the processed imageries were compiled into a list, which was then used for calculating the VHI. Individual and global Normalized Difference Vegetation Index (NDVI) and Land Surface Temperature (LST) were measured by the following equations.

Red, Near-Infrared (NIR) and Thermal Infrared (TIRS) bands. Where Red and NIR were used for NDVI, and the TIRS band was utilized for LST calculation.

$$NDVI = \frac{NIR - Red}{NIR + Red}$$

Where, *NIR* is Near-Infrared and Red is the red band of the satellite image. The Red and NIR bands for Landsat 5 and 7 were Band 3 and Band 4, respectively, and for the Landsat 8 and Landsat 9 they were Band 4 and Band 5, respectively.

The LST was calculated from the TIRS band of Landsat satellite images. This TIRS band is Band 6 for Landsat 5 and 7 and Band 10 for Landsat 8 and 9. After using the cloud- and shadow-masking in the TIRS band, a default scaling factor was applied to get the Top of Atmosphere (TOA) brightness temperature.

$$LST_K = (DN \times 0.00341802) + 149.0$$

Where, *DN* is the digital number of a pixel. This equation provided the land surface temperature in the unit of Kelvin, which was converted into Celsius by subtracting 273.15 from the Kelvin temperature.

$$LST_{\circ C} = LST_K - 273.15$$

The Vegetation Condition Index (VCI) and Temperature Condition Index (TCI) were eventually derived from NDVI and LST because VHI requires VCI and TCI for its measurement.

$$VCI = \frac{NDVI_{Current} - NDVI_{min}}{NDVI_{max} - NDVI_{min}} \times 100$$

Where, $NDVI_{Current}$ was the value of NDVI from a specific month, $NDVI_{min}$ and $NDVI_{max}$ were the historical value of, respectively, NDVI minimum and maximum from multiple time periods. Then, the resultant VCI was multiplied by 100 to make the range from 0 to 100. A VCI value near to 0 indicates that vegetation is not in good condition, whereas a value near 100 refers to a healthy vegetation condition. The *TCI* takes land surface temperature for its calculation.

$$TCI = \frac{LST_{max} - LST_{current}}{LST_{max} - LST_{min}} \times 100$$

Where, $LST_{Current}$ was the value of LST from a specific month, and LST_{min} and LST_{max} were the historical value of, respectively, the LST minimum and maximum from multiple time periods. Then, the resultant VCI was multiple by 100 to make the range from 0 to 100. A VCI value near to 0 indicates dry conditions, whereas a value near 100 refers to wet conditions. Then, the *VHI* was calculated using the following equation, combining both *VCI* and *TCI*.

$$VHI = \alpha \times VCI + (1 - \alpha) \times TCI$$

Where, α was the constant value of VHI; generally, the value for α is 0.5. *VCI* and *TCI* are vegetation and temperature conditions, respectively, which were calculated previously. The VHI resulted in a range from 0 to 100 where, a VHI value near to 0 indicates extreme drought conditions and a value near 100 refers to no-drought conditions. A more specific range of agricultural drought conditions from VHI is given in Table 3. This process was first run in GEE to get the annual VHI for pre-monsoon season and then again for post-monsoon period.

Afterwards, the affected areas from agricultural drought were computed for each drought category (Table 3) from 2000 to 2024 for both pre-monsoon and post-monsoon seasons. The classes of drought for VHI were chosen to be similar to SPEI to make the cross-tabulation between them. The area was calculated by summing up the pixels of a specific category for a particular year. The number of pixels was multiplied by 900 (pixel size 30 m×30 m) to convert into square meters and then divided by 1,000,000 to convert the area into square kilometers. Thus, the yearly drought-affected area of five drought categories was calculated for both the pre-monsoon and post-monsoon season.

Time series analysis of VHI

The time series analysis of VHI was completed using the Mann–Kendall Test. After the calculation of VHI, the time series data were prepared from the yearly mean value of VHI. The mean value for a season of a year was calculated using the Calculate Statistics tool in ArcMap. Then, with these values, a spreadsheet was created that includes a column for the year for which VHI is calculated and a column for the VHI mean value of pre-monsoon and post-monsoon. The Mann–Kendall Test was run in Jupyter Notebook using the created spreadsheet. The Mann–Kendall was already installed in the paymannkendall package of Python. The result from this time series analysis reveals the trend of VHI, statistically significant (p), Sen's slope and so on.

Drought frequency

The agricultural drought frequencies of the eight districts of Rajshahi division were calculated using a simple table generated from the VHI value. First, yearly VHI acquired data were prepared along with district name for pre-monsoon and post-monsoon seasons, separately. The frequency was counted by how many times one district faced a drought in all the selected twenty-five years. This was accomplished by checking whether or not a district had drought in a year and assigning 1 for "drought occurred" and 0 for "no drought occurred". If there was a drought, then it was checked which category the drought fell into. Since drought from VHI was categorized into five groups, a different rank was assigned for each of drought severity, where 1–20 was 1(Dry), 21–40 was 2 (Slightly dry), 41–60 was 3 (Normal), 61–80 was 4 (Slightly wet) and 81–100 was 5 (Wet).

Comparison between SPEI and VHI

The drought comparison between SPEI and VHI was performed using a confusion matrix in SPSS. A spreadsheet with two columns for SPEI and VHI, including all the data from pre-monsoon and post-monsoon seasons, was created to make a confusion matrix. In SPSS, the Crosstabs tool was used to make the matrix table. The confusion matrix helped to assess how classifications of drought from SPEI and VHI agree with each other.

Results

Agricultural drought assessment for two seasons from VHI

The agricultural drought from VHI was categorized into five different groups, viz, 1–20, 21–40, 41–60, 61–80 and 81–100, where the classified groups demonstrate dry, slightly dry, normal, slightly wet, and wet categories of drought, respectively.

Agricultural drought was found to be widespread throughout the Rajshahi division during the pre-monsoon season, as shown in Figure 3. From

Table 3. Category of agricultural drought from VHI

VHI range	Drought class	Class number	Vegetation conditions
0 to 20	Dry	1	Very poor health
21 to 40	Slightly Dry	2	Poor health
41 to 60	Normal	3	Fair vegetation
61 to 80	Slightly Wet	4	Good vegetation
81 to 100	Wet	5	Excellent vegetation

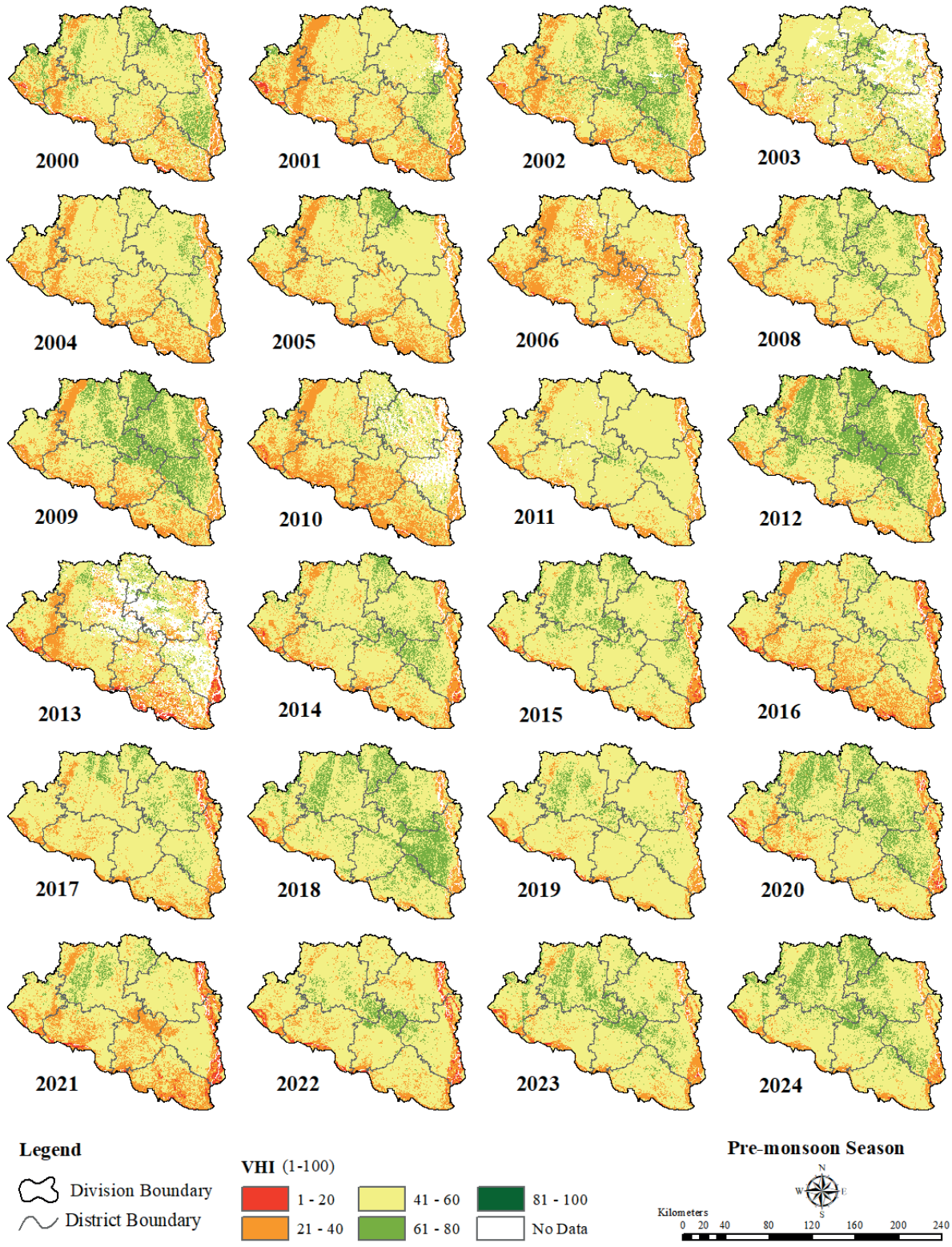

Fig. 3. Agricultural drought by VHI during pre-monsoon season

2000 to 2024, an extensive area was identified as exhibiting slightly dry and normal conditions of drought using the VHI method. In 2000 and 2001, the dry category of drought was recorded in the western and south-central zones of Rajshahi, demonstrating low vegetation conditions. A remarkable improvement in drought occurred in 2002, especially in the central to north-eastern part of the region, where vegetation conditions were classified as slightly wet. However, slightly dry to normal conditions remained in the east and south sides of the division. A similar pattern of drought conditions was found for the years 2003, 2004 and 2005. Most of the area was classified as having normal conditions; slightly dry conditions were also present in the southern, south-eastern and south-western parts in all three years. The eastern region also faced a slightly dry situation during 2004 and 2005. This "slightly dry" category of drought was extended to central and western areas, and dry conditions were marked at the southern zone of the region in 2006. The VHI map of 2008 and 2009 demonstrates rising vegetation conditions, particularly in the central, northern and eastern parts. In 2008, slightly wet conditions were dispersed, but this class of vegetation condition was much more widespread in 2009. In 2010, the healthier condition in vegetation suddenly decreased, and conditions were slightly dry and normal drought, even dry in some locations of the south-west. A recovery from slightly dry to normal drought conditions was prominent in 2011, and again, a dramatic improvement in vegetation occurred in the following year, reaching a vegetation condition of "slightly wet". The drought status was nearly the same from 2013 to 2016 across the region. Slightly wet vegetation conditions were found scattered in different areas, with the presence of normal to slightly dry drought in most areas of Rajshahi division. During these years, some areas also experienced the dry category of drought, and, in 2016, the total area affected by the slightly dry level of drought increased more compared to previous years. A recovery in vegetation condition was demonstrated in 2017, which continued to 2018, characterized by an expansion of vegetated area in northern and north-western regions. The drought conditions were varying from normal to slightly wet categories throughout 2019 and 2020, where vegetation in the northern part was in good condition, but drought was persistent in the southern zone. The "dry" and "slightly dry" categories of drought reoccurred in 2021, notably in the central and south-eastern part of Rajshahi division. In the last three years, during the pre-monsoon season, a slightly wet type of drought dominated in the central part of the region. Each year, this vegetation condition improved gradually and spread to northern and eastern regions. The drought conditions were mostly normal and slightly dry in some locations. The presence of the "dry" drought category was also visible in the northern and eastern parts, especially in 2022, which minimized at a certain level in 2024.

A large portion of the Rajshahi division experienced dry to slightly dry drought conditions in 2000 during the post-monsoon season (Fig. 4), where a wide area in the central to southern parts of Rajshahi showed below a 40 VHI value. Slightly dry conditions were also available in some areas of the northern and western parts of the region. In some areas, the VHI value was below 20, indicating dry conditions of drought in the same year. Though there was a little improvement in vegetation conditions in the following few years, demonstrating much of the land area remained in the "slightly dry" to "normal" categories of drought.

The development of vegetation was mostly noticeable in the western and northern parts of the region from 2001 to 2009. However, this improvement had no pattern; rather, the improvement in vegetation conditions was different in different areas and at different times. In 2009, a significant number of areas were shown as belonging to the "slightly wet" drought category by VHI, demonstrating favorable vegetation conditions. Nevertheless, in that year, slightly dry to normal drought conditions were also found, particularly in the southern and south-eastern parts of the region.

During 2010 to 2018, excluding 2013, the drought conditions were mostly normal in almost all areas, with slightly dry conditions in some portions, and very small areas had dry drought conditions for vegetation. In 2013, most of the areas had slightly wet conditions, which were normal drought conditions in previous years. After that year, the slightly dry category of drought reappeared heavily during this season until 2018.

From 2019 to 2024, there was a higher interannual variability of drought severity across the region. During 2019 and 2021, significant portions of the region exhibited slightly wet vegetation conditions, and, in some areas, wet vegetation conditions were also found by VHI. Conversely, in 2020, 2022, 2023 and 2024, Rajshahi witnessed an increase in slightly

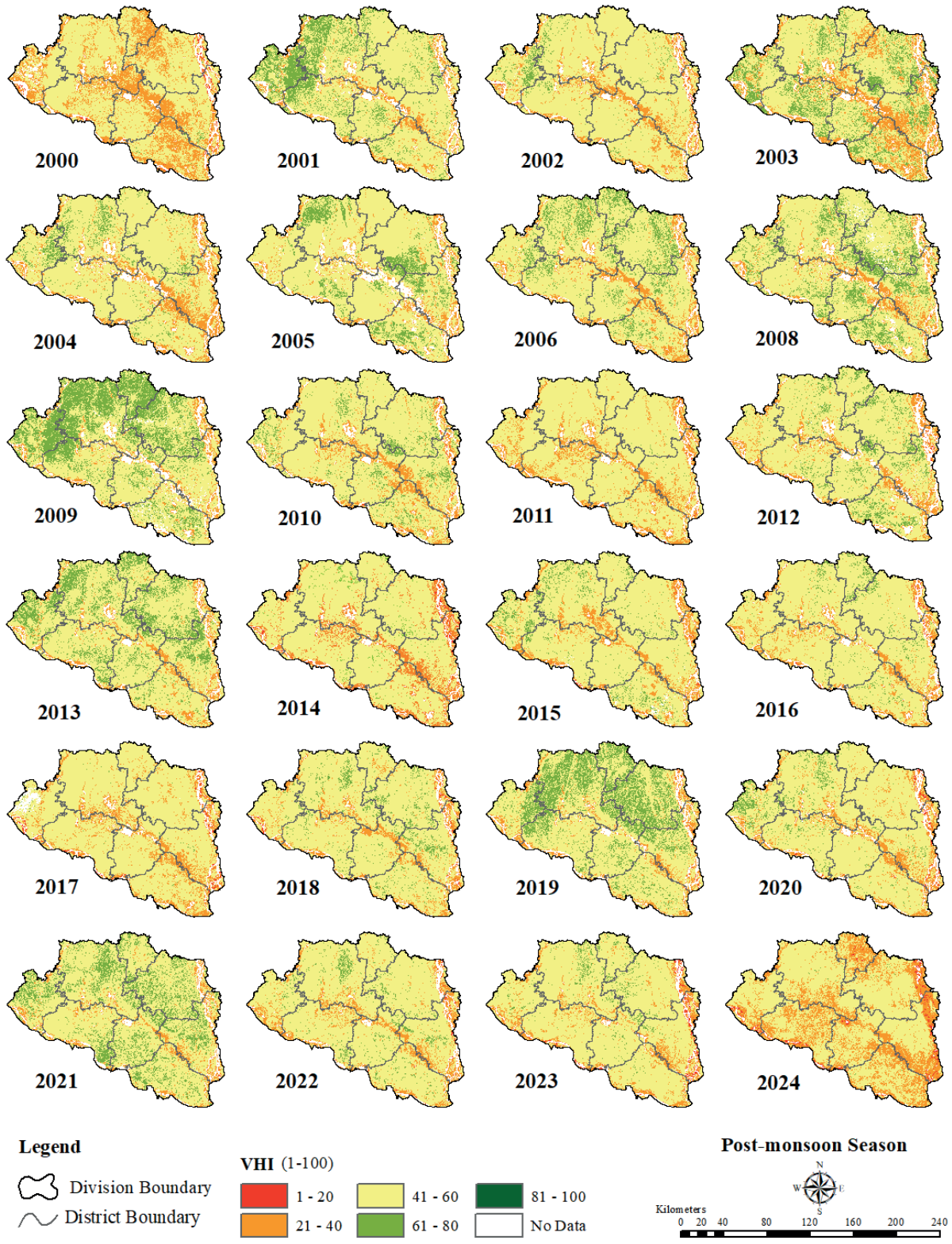

Fig. 4. Agricultural drought by VHI during post-monsoon season

dry and dry drought conditions. Particularly in 2024, drought stress on vegetation was higher and widespread across the region. During the post-monsoon season, the Rajshahi division consistently experienced dry to slightly dry conditions of drought, especially in the center and southern parts over the years. On the other hand, vegetation conditions are found to be normal to slightly wet levels of drought in the north and north-western part of the Rajshahi division.

Drought-affected area

The area affected by different levels of agricultural drought was calculated (Table 4) to understand the temporal variability of drought from 2000 to 2024. The level of severity was ordered as 1, 2, 3, 4 and 5 for "dry", "slightly dry", "normal", "slightly wet" and "wet", respectively. During the pre-monsoon season, the majority of the studied area was found to exhibit VHI of between 41 and 60 nearly every year. This demonstrated the normal category of drought severity, meaning the vegetation health was normal in condition.

In each year, the areal coverage was quite high for the "normal" level of drought conditions. Notably, areas of above 13,000 square kilometers (km²) more frequently underwent normal conditions, and, in 2011, such conditions obtained their greatest extent, at more than 17,000 km². Although most of the area was in regular (normal) drought conditions, some areas also faced dry conditions, having a VHI range of 1 to 20. The area coverage for dry conditions of drought is not so large, and the value fluctuated

Table 4. Drought-affected area during pre-monsoon and post-monsoon seasons

Year	Pre-monsoon area calculation (km²)					Post-monsoon area calculation (km²)				
	1	2	3	4	5	1	2	3	4	5
2000	133.073	3,434.963	13,665.902	2,149.160	0.000	145.593	5,696.529	12,868.885	54.750	0.000
2001	166.949	4,954.870	13,329.389	960.366	0.000	2.204	1,815.578	13,870.228	3,127.656	0.000
2002	61.826	4,140.803	12,026.095	3,343.143	0.044	59.082	2,492.609	16,026.593	519.924	0.000
2003	121.372	2,304.486	13,092.528	1,139.155	0.000	0.851	3,826.980	15,030.078	29.886	0.000
2004	0.918	4,082.093	15,178.833	481.812	0.054	0.431	2,856.344	14,903.944	1,045.777	0.038
2005	18.403	4,042.118	14,813.733	792.524	0.091	0.123	1,716.529	14,638.789	1,924.887	0.001
2006	61.335	5,939.037	13,132.247	19.819	0.014	2.598	2,270.957	14,607.723	2,419.102	0.048
2008	1.532	3,017.975	14,857.415	1,887.611	0.003	4.462	2,091.695	13,482.023	3,061.307	0.003
2009	19.080	4,027.454	11,041.883	4,682.134	0.005	1.115	1,350.843	11,328.132	5,903.198	0.016
2010	77.936	5,845.132	10,991.561	611.074	0.003	25.334	2,436.647	15,586.918	1,106.929	0.004
2011	3.198	2,127.629	17,214.038	287.215	0.000	41.198	3,171.857	15,851.010	37.570	0.000
2012	3.371	2,271.023	11,218.984	6,301.884	0.000	41.115	2,147.252	15,148.480	1,428.956	0.018
2013	480.602	4,012.050	9,341.971	843.701	0.000	4.852	1,683.881	13,965.987	3,645.373	0.084
2014	135.473	3,112.882	14,574.079	1,951.191	0.023	78.444	2,825.797	16,032.615	327.413	0.001
2015	183.128	1,688.584	15,726.589	2,257.452	0.003	44.951	2,275.636	16,196.186	963.910	0.072
2016	402.500	4,580.925	13,994.230	832.988	0.056	73.105	2,168.878	16,353.649	568.742	0.005
2017	146.793	2,517.200	16,029.885	1,169.237	0.017	163.055	2,842.628	15,896.638	37.211	0.068
2018	40.010	1,293.818	13,869.712	4,596.014	0.001	79.206	2,047.649	16,353.010	986.504	0.004
2019	103.710	1,605.417	17,117.247	1,008.395	0.000	44.535	1,560.343	12,641.285	4,958.131	0.010
2020	254.406	2,102.298	14,196.080	3,341.330	0.004	110.269	2,464.090	15,781.688	815.962	0.046
2021	527.598	4,487.597	13,980.614	812.707	0.004	6.506	1,504.482	14,183.275	3,617.456	0.000
2022	430.862	2,459.341	15,917.853	1,038.420	0.000	54.616	2,257.856	16,250.045	762.700	0.008
2023	111.091	1,980.761	15,319.345	2,499.574	0.000	205.964	2,135.390	16,451.384	585.156	0.005
2024	62.813	1,556.409	14,603.692	3,674.480	0.000	314.042	5,954.521	13,580.188	21.326	0.013

Citation: Bulletin of Geography. Physical Geography Series 2026, 30, http://doi.org/10.12775/bgeo-2026-0004

heavily from year to year. For instance, the area that exhibited the dry category of drought was 0.918 km^2 in 2001, but in 2021 this area extended to 527.598 km^2, though no linear trend was noted in drought area changes. These abrupt changes in drought conditions show that the area underwent severe drought conditions for the selected 24 years.

After the "normal" level drought conditions, slightly dry categories of drought (VHI 21 to 40) were calculated to be more common than "slightly wet" vegetation conditions. Year-to-year variations in drought-affected area were also visible for these slightly dry situations. The minimum and maximum areas affected by slightly dry drought were 1,293.818 km^2 in 2018 and 5,939.037 km^2 in 2006, respectively. In turn, the "slightly wet" conditions (VHI 61 to 80) indicating no agricultural drought situation encompassed its greatest area in 2012 (6,301.884 km^2).

The vegetation conditions at the time of the post-monsoon season were found to be better, in contrast to the previous season. Similar to the pre-monsoon season, the highest area coverage for this season was for normal drought conditions for the entire year. In 2023, they covered an area of 16,451.384 km², which was the largest of all study years, and in none of the years did the area go below 11,000 km². There was also an increase in drought variability in that particular season, compared to the previous few years. In 2024, slightly dry conditions of drought covered their largest area of any year in the study period, at 5,954.521 km². In the same year, exactly 314.042 km² of area was found to be dry, which is also the peak of the dry category of drought. This indicates a sharp expansion of the drought trend for the dry category over the years, as past years covered a comparatively small area.

In some years, the VHI value was even very near to 0. For example, in 2005, it was just 0.123 km^2. The table demonstrates that there was significant variability in the slightly wet category of drought during the post-monsoon season. The largest area, almost 6,000 km², was recorded during 2009 for this level of vegetation condition. This may be because the monsoon had just visited that area, increasing the moisture content in the soil as a result. Nevertheless, the situation was not consistent because, in the later part of the study period, the area with slightly wet conditions was getting smaller, suggesting that drought severity was increasing as the year passed. It was discovered that the wet category of VHI (81–100) was not recorded across either of the seasons. This absence represents that vegetation conditions were not in optimal situations, hence under normal conditions during the pre-monsoon and post-monsoon seasons. Moreover, the Rajshahi division encountered dry to slightly dry drought conditions throughout the year, and the risk was exacerbated because of the expansion of drought occurrences in these drought categories. The wet vegetation conditions were zero or almost zero km^2 during pre-monsoon and post-monsoon seasons in most of the years, which indicates that Rajshahi division had a minimal amount of vegetation that was in favorable conditions from 2000 to 2024.

Trend analysis of VHI-provided agricultural drought

The trend analysis shown in Table 5 was conducted using the Mann–Kendall (MK) test from the

Table 5. Trend analysis of drought from VHI using Mann–Kendall test

Parameters	Pre-monsoon	Post-monsoon
trend	No trend	No trend
h	False	False
p	0.078	0.785
z	1.761	0.273
Tau	0.261	0.043
s	72.0	12.0
var_s	1625.330	1625.330
slope	0.167	0.021
intercept	46.358	49.982

yearly averaged drought data provided by VHI. The long-term pattern in the state of vegetation was assessed by this MK trend analysis for the two selected seasons of the Rajshahi division over the 24 years. A number of core statistics, such as p-values, Sen's slope, Z-scores and Kendall's Tau can be concluded from the MK trend analysis. The result from the trend analysis indicates that, statistically, there were no substantial variations of the VHI value in any of the pre-monsoon or post-monsoon seasons. According to the test, the p-value for the pre-monsoon season was calculated to be 0.078, which is somewhat beyond the conventional level of significance (0.05). The finding was therefore merely suggestive, since statistically no significant trend was present there; the null hypothesis cannot be rejected. However, a slightly positive relationship between the values of VHI during the 24 years existed. This correlation and correspondence of Z score was about 1.76, revealing that there is a slightly upward trend in the VHI throughout the study period. However, with the significance level at 5%, it is not robust enough to achieve statistical importance. The estimated value of Kendall's Tau was 0.2609 for the pre-monsoon period, indicating the intensity as well as the direction of the linear pattern over the years. The Tau values suggested that the vegetation health is likely to improve at some level over time because Tau values ranging from 0.2 to 0.3 are often seen as reflecting a weak to somewhat positive relationship. The Sen's slope is a reliable measure of changes, which demonstrates that, during the pre-monsoon season, the VHI rose by ~0.17 units annually, as the Sen's slope was calculated at 0.166 during that season. At the starting point of the research period, the estimated value of VHI was 46.36, calculated by the intercept, which showed a point of reference for how trends changed over time. The S-statistic and variance were measured as 72 and 1625.33, respectively. These two parameters are essential to determine the Z-score and illustrate how many positive differences are greater than negative variations in the given time. The p-value from the MK test for the post-monsoon season was higher, as with the pre-monsoon season. The p-value was calculated as 0.7885, which significantly exceeded the threshold level, hence evidencing the lack of statistically substantial trends over the post-monsoon period. The Z-score was obtained as 0.273, confirming that the change in VHI over time was minimal, being near to zero. A very little positive correlation within VHI and year was suggested by the Kendall's Tau value, which was 0.0435.

The Sen's slope value was only 0.0208, which indicated that, each year, the vegetation health condition was improving negligibly. It was likely that the slightly higher value of intercept for VHI of pre-monsoon should be attributed to the vegetation being healthier compared to pre-monsoon. Moreover, there was no obvious trend in VHI over the 24 years as determined by the S-statistic, and the value for post-monsoon was 12, which was considerably lower than it was in pre-monsoon.

Figure 5 also illustrates the yearly trend of vegetation condition assessed by VHI during pre-monsoon and post-monsoon seasons. The line graph shows how the agricultural drought has changed from 2000 to 2024 over the Rajshahi division in both seasons. The values of the VHI revealed a significant amount of interannual fluctuation during the pre-monsoon season, also reflecting a progressive rising trend throughout the 24 years. During the years 2006 and 2012, the average VHI dropped to nearly 40, which reflects the possibility of stress on vegetation

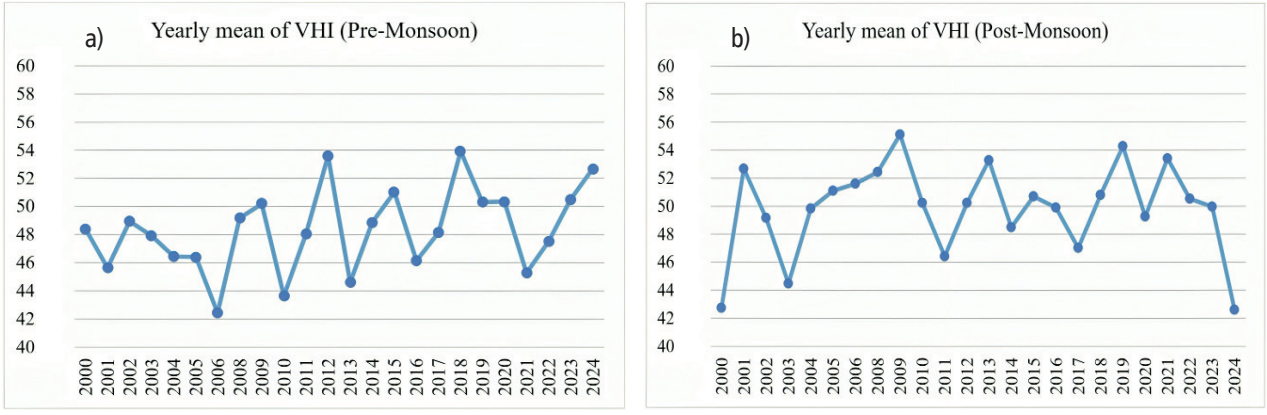

Fig. 5. Line graph showing the VHI mean value in different years: (a) during pre-monsoon, (b) during post-monsoon

Citation: Bulletin of Geography. Physical Geography Series 2026, 30, http://doi.org/10.12775/bgeo-2026-0004

health. But in 2012 and 2018, the situation was different. The average value of VHI was nearly 55 in both years, which means that the health of the vegetation was in normal condition. In 2021 the VHI value dropped, but then it began to rise and reached around 53. This showed that the conditions of vegetation were improving gradually during pre-monsoon. By contrast, the post-monsoon had a different pattern on the VHI value. In the earlier period of time, the mean VHI value demonstrated a significant increase from 2000 to 2009 and, in that year, the VHI reached its peak (of 55) during the post-monsoon season. After that year, the average values of the VHI began to vary without exhibiting a persistent rising or negative trend, ultimately remaining within a range that was quite steady until around 2021. In the years after 2021, the graph depicts a distinct decreasing trend, ending in an abrupt fall in 2024 and the lowest VHI value of 42.61 was measured for the post-monsoon season. Moreover, the graph demonstrates that, although the pre-monsoon VHI has shown a sign of steady recovery and improvement, the post-monsoon VHI has declined, especially in the most recent years, illustrating seasonal disparities in the response of vegetation over time.

The frequency of agricultural drought was analyzed based on the five drought severity categories of VHI over eight districts of the Rajshahi division. Table 6 presents the number of drought occurrences in a specific drought category for selected districts throughout the 24 years. Drought variability was noticeable, specifically in dry drought conditions (class 1) during the pre-monsoon season. With 24 occurrences of agricultural drought, Chapai and Sirajganj districts experienced the driest drought conditions. Rajshahi (23) and Pabna (23) came in a close second in dry drought frequency. Natore witnessed 22 and Bogra had 19 occurrences of dry drought conditions, which was also a relatively high drought frequency. Naogaon experienced less frequency of dry drought conditions, at only six occurrences within 24 years. But Joypurhat district was not affected by the dry drought situation in any of the years from 2000 to 2024, indicating a considerably stable vegetation condition. Throughout all districts, class 2 was consistently high, presenting 24 occurrences of drought out of the 24 years. This suggested that, in the pre-monsoon season, each of the districts experienced a slightly dry category of drought on vegetation conditions. During the post-monsoon season, the frequency of slightly dry conditions of vegetation was exactly the same as pre-monsoon. From 2000 to 2024, class 2 drought occurred in all years for all eight districts. Notably, there were significant variations for class 1 drought severity or dry agricultural drought conditions. In the pre-monsoon season, Chapai and Sirajganj districts exhibited a high frequency in the dry category of drought; however, for the post-monsoon season, Sirajganj maintained the consistency in dry drought conditions, recorded 24 times. Bogra also faced dry conditions frequently – 21 times within 24 years.

Occurrences of dry drought in this season reduced from 24 to 17 in Chapai, from 22 to 18 in Natore, from 23 to 21 in Pabna and from 23 to 20 in Rajshahi. This small decline in drought frequency showed that drought hazards were constant in these areas. But different things happened in Naogaon, where the frequency of dry drought conditions in the post-monsoon season was double (6 to 12) that of the pre-monsoon season. In the post-monsoon

Table 6. Frequency of agricultural drought during pre-monsoon and post-monsoon

Districts	Pre-monsoon drought frequency					Post-monsoon drought frequency				
	1	2	3	4	5	1	2	3	4	5
Bogra	19	24	24	24	2	23	24	24	24	2
Chapai	24	24	24	24	0	17	24	24	24	5
Joypurhat	0	24	24	24	0	2	24	24	21	1
Naogaon	6	24	24	24	2	12	24	24	24	11
Natore	22	24	24	24	0	18	24	24	24	2
Pabna	23	24	24	24	2	21	24	24	24	7
Rajshahi	23	24	24	24	8	20	24	24	24	10
Sirajganj	24	24	24	24	5	24	24	24	24	4

season, Joypurhat experienced a low frequency of class 1 drought, at exactly 2 occurrence within 24 years. Classes 3, 4 and 5 represented normal, slightly wet and wet conditions of vegetation, respectively, which were excluded during the drought frequency calculations

Comparison between SPEI and VHI

The confusion matrix (Table 7) comparing SPEI and VHI from 2000 to 2025 during the pre-monsoon season showed that the categories of drought from meteorological (SPEI) and agricultural (VHI) indices were moderately aligned with each other across the study region. Approximately 30% of the total 21,351 pixels corresponded to the same drought categories identified by both SPEI and VHI. The normal drought conditions from both SPEI and VHI had the strongest diagonal alignment with each other; 5,300 pixels fall into this category of vegetation conditions. The other pixels of normal conditions, found by SPEI, went to slightly dry (1,431 pixels), slightly wet (808 pixels), and dry (102 pixels) categories with the VHI method. The SPEI identified 4,305 pixels for the dry drought conditions, where most of the pixels (2,990) were found to represent normal conditions using the VHI calculation. Only 34 pixels matched the dry drought conditions from both the SPEI and VHI drought assessment methods. The Kappa coefficient and Pearson correlation were very low, –0.0374 and –0.0227, respectively, confirming a similar pattern. However, the linear correspondence and categorial agreement between SPEI and VHI was less favorable.

The biggest percentage of misinterpretation occurred when 6,864 pixels were categorized under normal conditions using the VHI but SPEI found it as slightly dry conditions of drought. From the 8,933 pixels, only 1,151 pixels matched as a slightly dry category of drought in both SPEI and VHI methods. Some pixels of slightly dry from SPEI were split into dry (24 pixels) and slightly wet (894 pixels) drought categories of VHI. In both of the drought calculation methods, the number of pixels for slightly wet areas was very few, at just 235 pixels in total, but only 64 pixels for SPEI and VHI aligned together at this level of drought. Though there were some pixels for wet according to the SPEI, the VHI nevertheless did not demonstrate anything for these conditions of vegetation. Therefore, these 237 pixels of wet from SPEI belonged to other categories of drought calculated by VHI. In general, during the pre-monsoon season, SPEI and VHI typically agreed with each other's measurement, but the relationship was very weak for dry, slightly dry and slightly wet drought categories.

A total of 21,142 pixels were used to create a cross-tabulation from SPEI and VHI during the post-monsoon season. Table 8 reveals that there were only a small number of pixels aligned with the two indices in this season. Notably, the normal category of drought was consistently identified by both SPEI and VHI indices. It was determined that 7,053 pixels were classified as the normal drought category by SPEI and VHI, indicating the maximum diagonal similarity, which was also the largest pixel count for the pre-monsoon season under this drought category. However, several pixels identified as normal conditions of drought by SPEI were classified into other categories by VHI; viz., 1297 pixels were considered slightly dry, 694 pixels slightly wet, and 35 pixels dry. The very weak alignment between SPEI and VHI was observed for dry and slightly dry categories of drought. Although 3,125 pixels were marked as dry using SPEI, just four pixels were equally identified as dry by both indices, and the

Table 7. Confusion matrix between SPEI and VHI in pre-monsoon season

SPEI and VHI pre-monsoon cross-tabulation						
		VHI				
		Dry	Normal	Slightly dry	Slightly wet	Total
SPEI	Dry	34	2,99	921	360	4,31
	Normal	102	5,30	1,43	808	7,64
	Slightly dry	24	6,86	1,15	894	8,93
	Slightly wet	1	159	11	64	235
	Wet	1	183	26	27	237
Total		162	15,50	3,54	2153	21,35

Citation: Bulletin of Geography. Physical Geography Series 2026, 30, http://doi.org/10.12775/bgeo-2026-0004

Table 8. Confusion matrix between SPEI and VHI in post-monsoon season

SPEI and VHI post-monsoon cross-tabulation						
		VHI				
		Dry	Normal	Slightly dry	Slightly wet	Total
SPEI	Dry	4	2,48	397	244	3,13
	Normal	35	7,05	1,30	694	9,08
	Slightly dry	24	6,71	962	751	8,44
	Slightly wet	2	115	40	0	157
	Wet	8	211	118	1	338
Total		73	16,57	2,81	1,69	21,14

majority of the pixels were categorized as normal conditions with VHI. The Pearson correlation was near to zero, at ~0.0046, and the Kappa coefficient was also very low, at around –0.0188 during this season. These statistical outcomes indicated there was no meaningful linear relationship and very weak overall agreement between SPEI and VHI during post monsoon season.

Discussion

The analysis of agricultural drought showed a substantial variability in drought distribution, frequency and severity within years and seasons alike. However, the interpretation of drought for Rjashahi division requires factors like the region's socio-economic status, agricultural practice and financial conditions. Climatic pattern is another very important factor to consider for vulnerability measurement of local people. The drought condition in Bangladesh, particularly in the north-western part, is firmly influenced by low precipitation, high temperature and evapotranspiration. The combination of these weather patterns creates stress on the moisture content of soil. Human-induced factors such as excessive use of groundwater for irrigation and different land-use practices can influence the drought casualties of the Rajshahi division. Negligible agreement between meteorological and agricultural drought, with considerable misclassifications in dry and slightly dry drought conditions, but a robust relationship in normal conditions of vegetation, was established by the confusion matrix. A study (Mahmud et al. 2021) also found that there is no significant relationship between meteorological drought and agricultural drought. During this study, a large number of pixels were found as normal drought conditions in SPEI, but VHI demonstrated them as a slightly dry category of drought, suggesting the situation may be normal from a meteorological perspective, but has stress on vegetation health conditions resulting in agricultural drought.

The drought analysis from VHI can be helpful for policymakers to make decisions about which areas are constantly suffering from dry or slightly dry categories of drought and what kind of techniques can be applied to mitigate such drought conditions. However, drought analysis using VHI was effective for Rajshahi division, though applying the same method for different regions may require that adjustments be made. Previous research (Gurdak et al. 2021) revealed the difficulties in developing a common drought monitoring method across different regions, because the climatic pattern and agricultural practices vary from region to region. Bangladesh also has similar constraints due to the seasonal crop cycles and different land-use practices in different regions, which can bring uncertainty while analyzing agricultural drought with a single method. Therefore, it is required to integrate the local parameters with the existing drought analysis method for better accuracy. Drought effects are not limited to the local scale, but, rather, can exacerbate at the regional or even national level. Local-level crop production data on different crop types can be integrated with VHI results to see the actual scenario of drought impact by understanding the extent of drought severity, which can damage some or all of crop production for a particular crop in a specific region. Although the occurrence of agricultural drought cannot be controlled, drought can be managed to mitigate the consequences.

Finding the factors that directly or indirectly led to drought conditions would be a great work to do for managing agricultural drought in an area.

Although VHI is one of the robust and reliable methods for assessing agricultural drought from optical remote sensing data, this study experienced some drawbacks while analyzing drought. The primary and most common challenges were cloud coverage, which led to the omission of some portions of the image after removing the cloudy pixels and even the omission of an entire year (2007). Furthermore, this study did not go through any ground-truth validation, which may affect the accuracy of drought assessment. Additionally, adding land use and land cover with VHI probably gives a better understanding of agricultural drought assessment, because, during this study, some areas showed high severity of drought in the sand bar (locally known as "char"). The study focused on the Rajshahi division only; in a similar way, other divisions or districts of Bangladesh can be analyzed where the population mostly relies on agricultural activities.

Conclusion

This study examined agricultural drought utilizing VHI, a standard index for drought assessment. The region for drought evaluation was Rajshahi (a north-western division of Bangladesh) from 2000 to 2024 (excluding 2007). The result from VHI was compared with meteorological drought from SPEI. The result demonstrates that, during the study period, Rajshahi underwent frequent pre- and post-monsoon drought. Each year, the agricultural drought visited this region with different intensity. However, in most of the areas, drought was more severe and extensive during the pre-monsoon season. Districts like Chapai, Pabna, Sirajganj and Rajshahi faced an extreme drought event in almost all years. Slightly dry to dry drought conditions were found during 2000, 2001, 2004, 2005, 2006, 2010, 2011, 2014, 2016, 2017, 2019, 2020, 2021 and 2024, with a frequent drought event in the central part. But in 2009, 2012 and 2018, vegetation conditions improved in the pre-monsoon and post-monsoon seasons. Most of the regions had slightly dry drought conditions in both seasons, according to VHI method. However, dry drought conditions also occurred throughout the study period but in a small area. Although the vegetation conditions were improving gradually from 2021 to 2024 in the pre-monsoon season, the scenario was completely the inverse during the post-monsoon season. The frequency analysis of drought also disclosed much variation, particularly in dry drought conditions. Chapai and Shirajganj witnessed the dry category of drought in every year for both seasons. Conversely, this frequency was very low for Joypurhat and Naogaon districts. The Mann–Kendall trend analysis for VHI found no significant trend of drought occurrence. The influence of meteorological drought on agricultural drought, showed by a confusion matrix, suggested that there was no strong relationship between SPEI and VHI. Although SPEI had some influence on VHI, meteorological drought is not the only factor that influences the extent and intensity of agricultural drought of a region.

Disclosure statement

No potential conflict of interest was reported by the authors

Author contributions

Study design: RR, ARM; data collection: ARM; statistical analysis: ARM; result interpretation: NNJ, RR; manuscript preparation: NNJ, ARM; literature review: ARM.

References

AKTER KS and RAHMAN MM, 2012, Spatio-Temporal Quantification and Characterization of Drought Patterns in Bangladesh. *Journal of Water and Environment Technology* 10(3): 277–288. DOI: https://doi.org/10.2965/jwet.2012.277.

ALAM S, ROY LC and AUTHOR C, 2024, ASSESSING LONG-TERM CLIMATE TRENDS IN RAJSHAHI DIVISION, BANGLADESH: AN

EXTENSIVE ANALYSIS OF METEOROLOGICAL DATA. *December*.

ALAMGIR M, SHAHID S, HAZARIKA MK, NASHRRULLAH S, HARUN S BIN and SHAMSUDIN S, 2015, Analysis of Meteorological Drought Pattern During Different Climatic and Cropping Seasons in Bangladesh. *Journal of the American Water Resources Association* 51(3): 794–806. DOI: https://doi.org/10.1111/jawr.12276.

ARANEDA-CABRERA RJ, BERMUDEZ M and PUERTAS J, 2021, Revealing the spatio-temporal characteristics of drought in Mozambique and their relationship with large-scale climate variability. *Journal of Hydrology: Regional Studies* 38. DOI: https://doi.org/10.1016/j.ejrh.2021.100938.

ARNELL NW, 2007, Climate change and drought. *Disaster Prevention and Management: An International Journal* 16(2): 51–66. DOI: https://doi.org/10.1108/dpm.2007.07316bag.005.

ASWATHI PV, NIKAM BR, CHOUKSEY A and AGGARWAL SP, 2018, Assessment and monitoring of agricultural droughts in Maharashtra using meteorological and remote sensing based indices. *ISPRS Annals of the Photogrammetry, Remote Sensing and Spatial Information Sciences* 4(5): 253–264. DOI: https://doi.org/10.5194/isprs-annals-IV-5-253-2018.

BARTOLD M, WRÓBLEWSKI K, KLUCZEK M, DĄBROWSKA-ZIELIŃSKA K and GOLIŃSKI P, 2024, Examining the Sensitivity of Satellite-Derived Vegetation Indices to Plant Drought Stress in Grasslands in Poland. *Plants* 13(16): 2319. DOI: https://doi.org/10.3390/plants13162319.

BAYABLE G and GASHAW T, 2021, Spatiotemporal variability of agricultural drought and its association with climatic variables in the Upper Awash Basin, Ethiopia. *SN Applied Sciences* 3(4): 1–20. DOI: https://doi.org/10.1007/s42452-021-04471-1.

BEGNA T, DANIELA NAOMI O-F, ARTURO AMED L-M, CAROLINA J-H, VICTOR SALVADOR C-G, ANDRES A-R and HERNANDEZ ALBERTO RM, 2022, IMPACT OF DROUGHT STRESS ON CROP PRODUCTION AND ITS MANAGEMENT OPTIONS. *International Journal of Research Studies in Agricultural Sciences* 8(12): 1–13. DOI: https://doi.org/10.20431/2454-6224.0812001.

BERG A and SHEFFIELD J, 2018, Climate Change and Drought: the Soil Moisture Perspective. *Current Climate Change Reports* 4(2): 180–191. DOI: https://doi.org/10.1007/s40641-018-0095-0.

BINTE MAHTAB S and MOSTAFA KHAN S, 2018, Changes in Historical Precipitation Extremes over Bangladesh. *International Journal of Scientific Engineering and Research* 6(9): 64–68. DOI: https://doi.org/10.70729/ijser18217.

BOHON C, 2024, Satellite Crop Monitoring: Track NDVI & VHI for Yield Forecasting. Available at: https://www.cropprophet.com/satellite-crop-monitoring-ndvi-vhi/.

CHENG M, LU X, LIU Z, YANG G, ZHANG L, SUN B, WANG Z, ZHANG Z, SHANG M and SUN C, 2024, Accurate Characterization of Soil Moisture in Wheat Fields with an Improved Drought Index from Unmanned Aerial Vehicle Observations. *Agronomy* 14(8). DOI: https://doi.org/10.3390/agronomy14081783.

COOK BI, MANKIN JS and ANCHUKAITIS KJ, 2018, Climate Change and Drought: From Past to Future. *Current Climate Change Reports* 4(2): 164–179. DOI: https://doi.org/10.1007/s40641-018-0093-2.

DABROWSKA-ZIELINSKA K, MALINSKA A, BOCHENEK Z, BARTOLD M, GURDAK R, PARADOWSKI K and LAGIEWSKA M, 2020, Drought model DISS based on the fusion of satellite and meteorological data under variable climatic conditions. *Remote Sensing* 12(18). DOI: https://doi.org/10.3390/RS12182944.

DAI A, ZHAO T and CHEN J, 2018, Climate Change and Drought: a Precipitation and Evaporation Perspective. *Current Climate Change Reports* 4(3): 301–312. DOI: https://doi.org/10.1007/s40641-018-0101-6.

DATA C, n.d., Weather Rajshahi Division in April 2026: Temperature & Climate. Available at: https://en.climate-data.org/asia/bangladesh/rajshahi-division-2265/r/april-4/.

FARMONAUT, 2024, EVI vs NDVI: Understanding the Key Differences in Vegetation Indices for Precision Agriculture. Available at: https://farmonaut.com/remote-sensing/evi-vs-ndvi-understanding-the-key-differences-in-vegetation-indices-for-precision-agriculture/.

FERDOUS M and BATEN M, 2012, Climatic Variables of 50 Years and their Trends over Rajshahi and Rangpur Division. *Journal of Environmental Science and Natural Resources* 4(2): 147–150. DOI: https://doi.org/10.3329/jesnr.v4i2.10165.

GAITÁN E, MONJO R, PÓRTOLES J and PINO-OTÍN MR, 2020, Impact of climate change on drought in Aragon (NE Spain). *Science of the Total Environment* 740: 140094. DOI: https://doi.org/10.1016/j.scitotenv.2020.140094.

GURDAK R, DĄBROWSKA-ZIELIŃSKA K, BOCHENEK Z, KLUCZEK M, BARTOLD M, NEWETE SW and CHIRIMA GJ, 2021, CROP GROWTH MONITORING AND YIELD PREDICTION SYSTEM APPLYING COPERNICUS DATA FOR POLAND & SOUTH AFRICA. *International Geoscience and Remote Sensing Symposium (IGARSS)*: 6564–6567. DOI: https://doi.org/10.1109/IGARSS47720.2021.9554744.

HABIBA U, HASSAN AWR and SHAW R, 2013, Livelihood Adaptation in the Drought Prone Areas

of Bangladesh. In: *Climate Change Adaptation Actions in Bangladesh*: 227–252. Springer, Tokyo. DOI: https://doi.org/10.1007/978-4-431-54249-0_13.

HAQUE M, HAQUE AKMM, ASFAQ M and FF S, 2019, Climate Change in Bangladesh: Effect versus Awareness of the Local People and Agencies of Rajshahi City. *Social Science Journal* 22.

IAFRATE L, ESPOSITO S and BELTRANO MC, 2017, Historical climatology research: The concept of "climate change" over time. *Italian Journal of Agrometeorology* 22(2): 53–64. DOI: https://doi.org/10.19199/2017.2.2038-5625.053.

ISLAM MS, HOSSAIN MZ and SIKDER MB, 2019, Drought adaptation measures and their effectiveness at Barind Tract in northwest Bangladesh: a perception study. *Natural Hazards* 97(3): 1253–1276. DOI: https://doi.org/10.1007/s11069-019-03704-2.

JIANG C, MA C, DUAN S, MIN X, ZHANG Y, LI D and ZHANG X, 2025, Monitoring of agricultural drought based on multi-source remote sensing data in Heilongjiang Province, China. *Journal of Integrative Agriculture*. DOI: https://doi.org/10.1016/j.jia.2025.04.027.

JIMÉNEZ-DONAIRE MDP, GIRÁLDEZ JV and VANWALLEGHEM T, 2020, Impact of climate change on agricultural droughts in Spain. *Water (Switzerland)* 12(11): 1–13. DOI: https://doi.org/10.3390/w12113214.

KAMRUZZAMAN M, HWANG S, CHO J, JANG MW and JEONG H, 2019, Evaluating the spatio-temporal characteristics of agricultural drought in bangladesh using effective drought index. *Water (Switzerland)* 11(12). DOI: https://doi.org/10.3390/W11122437.

KLOOS S, YUAN Y and CASTELLI M, 2021, Agricultural Drought Detection with MODIS Based Vegetation Health Indices in Southeast Germany. 1–24.

KUJ S and KAM C, 2021, Vegetation Condition Index based Agricultural Drought mapping over the past decade of Sri Lanka by utilizing the Satellite Remote Sensing. *March*: 65–71.

LOUKAS A, VASILIADES L and TZABIRAS J, 2008, Climate change effects on drought severity. *Advances in Geosciences* 17: 23–29. DOI: https://doi.org/10.5194/adgeo-17-23-2008.

M. MENEGBO E, 2024, Assessment of vegetation health index (VHI) using Modis data in rivers state, Nigeria. *International Journal of Advanced Geosciences* 12(2): 75–79. DOI: https://doi.org/10.14419/1w1pqg42.

MAHMUD T, SIFA SF, ISLAM NN, RAFSAN MA, KAMAL ASMM, HOSSAIN MS, RAHMAN MZ and CHAKRABORTY TR, 2021, Drought dynamics of Northwestern Teesta Floodplain of Bangladesh: a remote sensing approach to ascertain the cause and effect. *Environmental Monitoring and Assessment* 193(4): 1–19. DOI: https://doi.org/10.1007/s10661-021-09005-1.

MEASHO S, CHEN B, TRISURAT Y, PELLIKKA P and GUO L, 2019, Spatio-Temporal Analysis of Vegetation Dynamics as a Response to Climate Variability and Drought Patterns in the Semiarid Region, Eritrea. *Remote Sensing* 11(6): 724. DOI: https://doi.org/10.3390/rs11060724.

MONDOL MAH, ARA I and DAS SC, 2017, Meteorological Drought Index Mapping in Bangladesh Using Standardized Precipitation Index during 1981-2010. *Advances in Meteorology* 2017. DOI: https://doi.org/10.1155/2017/4642060.

MUKHERJEE S, MISHRA A and TRENBERTH KE, 2018, Climate Change and Drought: a Perspective on Drought Indices. *Current Climate Change Reports* 4(2): 145–163. DOI: https://doi.org/10.1007/s40641-018-0098-x.

MUSTAPHA M and ZINEDDINE M, 2024, Assessing the Impact of Climate Change on Seasonal Variation in Agricultural Land Use Using Sentinel-2 and Machine Learning. *Environmental Sciences Proceedings* 29(1): 51. DOI: https://doi.org/10.3390/ecrs2023-16365.

PEI W, FU Q, LI T, WANG P and HOU R, 2019, Study of the spatiotemporal variability in agricultural drought vulnerability based on a dynamic classification projection pursuit model. *Arabian Journal of Geosciences* 12(24). DOI: https://doi.org/10.1007/s12517-019-4949-0.

PEQUENO DNL, HERNÁNDEZ-OCHOA IM, REYNOLDS M, SONDER K, MOLEROMILAN A, ROBERTSON RD, LOPES MS, XIONG W, KROPFF M and ASSENG S, 2021, Climate impact and adaptation to heat and drought stress of regional and global wheat production. *Environmental Research Letters* 16(5). DOI: https://doi.org/10.1088/1748-9326/abd970.

PRODHAN FA, ZHANG J, BAI Y, PANGALI SHARMA TP and KOJU UA, 2020, Monitoring of drought condition and risk in bangladesh combined data from satellite and ground meteorological observations. *IEEE Access* 8: 93264–93282. DOI: https://doi.org/10.1109/ACCESS.2020.2993025.

SALITE D, 2019, Traditional prediction of drought under weather and climate uncertainty: analyzing the challenges and opportunities for small-scale farmers in Gaza province, southern region of Mozambique. *Natural Hazards* 96(3): 1289–1309. DOI: https://doi.org/10.1007/s11069-019-03613-4.

SANDEEP P, REDDY GPO, JEGANKUMAR R and KUMAR KCA, 2021, Monitoring of agricultural drought in semi-arid ecosystem of Peninsular India through indices derived from time-series CHIRPS

and MODIS datasets. *Ecological Indicators* 121: 107033. DOI: https://doi.org/10.1016/j.ecolind.2020.107033.

SHOLIHAH RI, TRISASONGKO BH, SHIDDIQ D, IMAN LOS, KUSDARYANTO S, MANIJO and PANUJU DR, 2016, Identification of Agricultural Drought Extent Based on Vegetation Health Indices of Landsat Data: Case of Subang and Karawang, Indonesia. *Procedia Environmental Sciences* 33: 14–20. DOI: https://doi.org/10.1016/j.proenv.2016.03.051.

SRUTHI S and ASLAM MAM, 2015, Agricultural Drought Analysis Using the NDVI and Land Surface Temperature Data; a Case Study of Raichur District. *Aquatic Procedia* 4: 1258–1264. DOI: https://doi.org/10.1016/j.aqpro.2015.02.164.

SULTANA MS, GAZI MY and MIA MB, 2021, Multiple indices based agricultural drought assessment in the northwestern part of Bangladesh using geospatial techniques. *Environmental Challenges* 4: 100120. DOI: https://doi.org/10.1016/j.envc.2021.100120.

SUN P, ZHANG Q, WEN Q, SINGH VP and SHI P, 2017, Multisource Data-Based Integrated Agricultural Drought Monitoring in the Huai River Basin, China. *Journal of Geophysical Research: Atmospheres* 122(20): 10,751-10,772. DOI: https://doi.org/10.1002/2017JD027186.

SUNNY F, MIAH MS, MIA MY and RIMI RH, 2021, Temporal Variability, Trends of Climatic Variables and Drought Analysis of Rajshahi and Sylhet District, Bangladesh. *Journal of the Asiatic Society of Bangladesh, Science* 46(2): 133–141. DOI: https://doi.org/10.3329/jasbs.v46i2.54409.

TONYALIOĞLU EE and ATAK BK, 2024, AGRICULTURAL DROUGHT ANALYSIS BASED ON REMOTE SENSING: THE CASE OF AYDIN, TURKIYE (Agricultural Drought Analysis Based on Remote Sensing: The Case of Aydin, Turkiye – in Turkish). *Turkish Journal of Forest Science* 8(2): 133–146. DOI: https://doi.org/10.32328/TURKJFORSCI.1508796.

VARGHESE D, RADULOVIĆ M, STOJKOVIĆ S and CRNOJEVIĆ V, 2021, Reviewing the potential of sentinel-2 in assessing the drought. *Remote Sensing* 13(17). DOI: https://doi.org/10.3390/rs13173355.

WILHITE DA, 1993, Drought Assessment, Management, and Planning: Theory and Case Studies. Kluwer Academic Publishers.

WU B, MA Z and YAN N, 2020, Agricultural drought mitigating indices derived from the changes in drought characteristics. *Remote Sensing of Environment* 244: 111813. DOI: https://doi.org/10.1016/j.rse.2020.111813.

WU T, ZHENG W, YIN W and ZHANG H, 2021, Spatiotemporal characteristics of drought and driving factors based on the grace-derived total storage deficit index: A case study in southwest china. *Remote Sensing* 13(1): 1–19. DOI: https://doi.org/10.3390/rs13010077.

YANG Z, DI L, YU G and CHEN Z, 2011, Vegetation condition indices for crop vegetation condition monitoring. *International Geoscience and Remote Sensing Symposium (IGARSS)*: 3534–3537. DOI: https://doi.org/10.1109/IGARSS.2011.6049984.

ZHAI J, KUMAR S, FISCHER T, WANG Y, SU B and ASIA S, 2020, Future drought characteristics through a multi-model ensemble from CMIP6 over South Asia. *Atmospheric Research* 246: 105111. DOI: https://doi.org/10.1016/j.atmosres.2020.105111.

Received 6 October 2025
Accepted 18 December 2025